Available online at www.sciencedirect.com
SCIENCE DIRECT
Carbohydrate Research 341 (2006) 650–662
Carbohydrate RESEARCH

Dynamics of water in supercooled aqueous solutions of glucose and poly(ethylene glycol)s as studied by dielectric spectroscopy

Madhusudan Tyagi[†] and S. S. N. Murthy[*]

School of Physical Sciences, Jawaharlal Nehru University, New Delhi 110 067, India

Received 17 August 2005; received in revised form 9 December 2005; accepted 28 December 2005
Available online 26 January 2006

Abstract—The dielectric behaviour of aqueous solutions of glucose, poly(ethylene glycol)s (PEGs) 200 and 600, and poly(vinyl pyrrolidone) (PVP) has been examined at different concentrations in the frequency range of 10^{6}–10^{-3} Hz by dielectric spectroscopy and by using differential scanning calorimetry down to 77 K from room temperature. The shape of the relaxation spectra and the temperature dependence of the relaxation rates have been critically examined along with temperature dependence of dielectric strength. In addition to the so-called primary (α-) relaxation process, which is responsible for the glass-transition event at T_g, another relaxation process of comparable magnitude has been found to bifurcate from the main relaxation process on the water-rich side, which continues to the sub-T_g region, exhibiting relaxation at low frequencies. The sub-T_g process dominates the dielectric measurements in aqueous solutions of higher PEGs, and the main relaxation process is seen as a weak process. The sub-T_g process was not observed when water was replaced by methanol in the binary mixtures. These observations suggest that the sub-T_g process in the aqueous mixtures is due to the reorientational motion of the 'confined' water molecules. The corresponding dielectric strength shows a noticeable change at T_g, indicating a hindered rotation of water molecules in the glassy phase. The nature of this confined water appears to be anomalous compared to most other supercooled confined liquids.

Keywords: Dielectric relaxation; Glass transition; Aqueous solutions; Glucose; Polyethylene glycols; Polyvinyl pyrrolidone

1. Introduction

Glassy carbohydrates are widely used for stabilization and encapsulation of foods, proteins and peptides, and in this context it is has been observed that the lower the water content, the better is the stability.[1–3] Also because of the increasing importance of carbohydrates in cryopreservation,[4,5] it has become very important to understand the dynamics of water (and its structure) in both the liquid and glassy states of the sugars, and other hydrogen-bonded liquids.

The dielectric relaxation technique is very widely used in this context because water has a large dipole moment. Systematic dielectric measurements have been made on aqueous solutions of poly(ethylene glycol)s (PEGs),[6,7] poly(vinyl pyrrolidone) (PVP),[6–9] monomeric alcohols,[10,11] glycols,[12,13] biopolymers,[14,15] amino acids[16] and carbohydrates[17,18] at room temperature and above. In these publications, it is observed that aqueous solutions of monomeric alcohols and lower PEGs, reveal only one relaxation process at room temperature, whereas aqueous solutions of PVP and higher PEGs tend to show two relaxation processes that are attributed to 'bound' water and 'free/loosely bound' water, respectively.[6]

However, almost all the aqueous solutions in their supercooled and glassy regimes[19–30] reveal again two relaxation processes: a relaxation process that freezes at T_g, and the other that is Arrhenius, continues to the sub-T_g region attributable to 'loosely bound/confined' water.[31] Interestingly, this sub-T_g process appears to be very similar in relaxation characteristics to that found by Chan et al.,[25] Noel et al.[26,27] and Moran and Jeffrey[28]

* Corresponding author. Tel.: +91 11 26704637; fax: +91 11 26717537; e-mail: ssnm0700@mail.jnu.ac.in
† Present address: Donostia International Physics Center, Paseo Manuel de Lardizabal, 4 San Sebastian 20018, Spain.

0008-6215/$ - see front matter © 2006 Elsevier Ltd. All rights reserved.
doi:10.1016/j.carres.2006.01.006

in aqueous solutions of glucose. It also appears to be very similar to the sub-T_g process observed by Pathmanathan and Johari[32] in aqueous solution of poly(2-hydroxyethyl methacrylate), (PHEMA), and interestingly enough it is also similar to the relaxation of 2D-layered water molecules of Bergman and co-workers.[33,34] In all the above cases, the activation energy of the sub-T_g process is in the range of 45–65 kJ/mol.

In order to get a better insight into the sub-T_g process, it is desirable to perform ultra low-frequency measurements in order to critically examine the T-dependence of peak loss frequency f_m and the dielectric strength $\Delta\varepsilon$

Table 1. Details of the parameters of process II

Sample	T_g (K) (DSC)	Temp range (K)	$\log f_{m,0}$ (Hz)	E_{II} (kJ/mol)	Range of		
					$\Delta\varepsilon_{II}$	α_{HN}	β_{HN}
Glucose–water ($x = 0.15$)	232.5[a]	206–253	17.97	63.47	5.15–16.8	0.64–0.653	0.70–0.90
Glucose–water ($x = 0.25$)	206.4[a]	189–226	14.64	47.52	9.65–18.4	0.555–0.65	0.626–0.92
PEG200–water ($x = 0.267$)	178.9	180–224	17.16	54.80	27–30.2	0.455–0.340	1–1
PEG600–water ($x = 0.404$)	194.4	176–194	17.29	52.56	28.10–30.0	0.443–0.465	1–1
PVP–water (x[b] $= 0.5$)	193 ± 6	174–241	21.87	69.88	24.4–32.2	0.44–0.41	1–1

[a] Taken from Ref. 37.

[b] This was the initial concentration. The exact concentration of this sample during cooling, is not known as a part of the sample was found to crystallize.

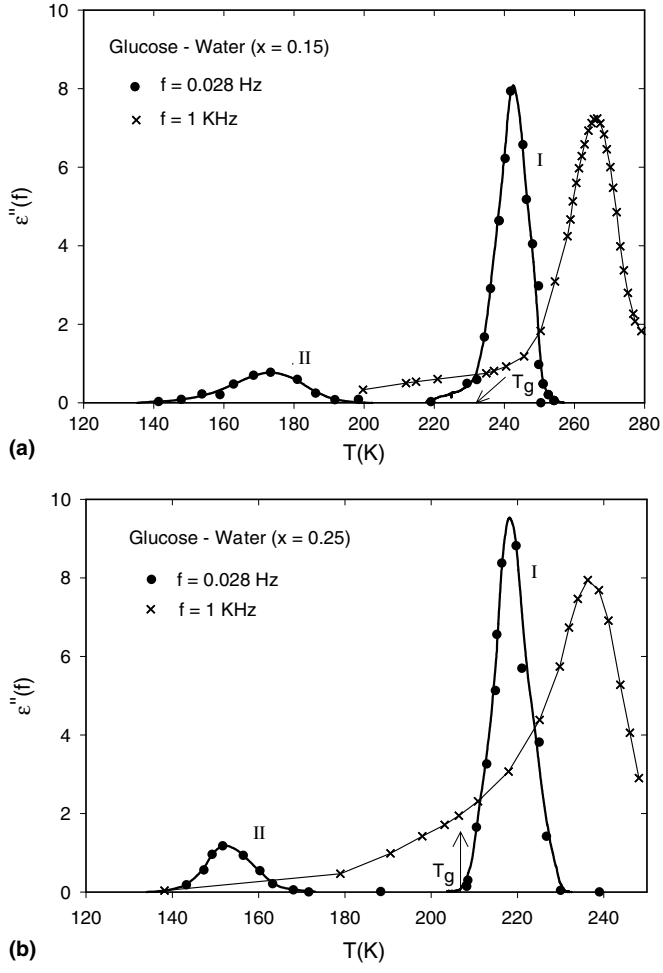

Figure 1. Temperature variation of the imaginary part of dielectric constant in glucose–water for (a) $x = 0.15$ and (b) $x = 0.25$ at test frequencies of 0.028 Hz and 1 kHz. The experimental points for 1 kHz are not shown in the diagram for the sake of clarity. The lines drawn through the points are guide to the eye.

of the sub-T_g process across T_g. It is with this in mind that we have performed this study.

2. Experimental

The water used in this study was of HPLC grade and was obtained from E. Merck, India. The sources of the other chemicals used in this study are as follows: D-glucose (Qualigens, India, AR grade); polyethylene glycol (PEG) 200 (E. Merck, India, AR Grade); PEG600 (E. Merck, India, AR Grade); methanol (MeOH) (C.D.H. India, HPLC grade); propylene glycol (PG) (s.d. Fine Chemicals, India, AR grade); and poly-(vinyl pyrrolidone) (PVP) (C.D.H. India, approx. molecular weight of 4000). The samples were used without any further purification.

Three kinds of measurements were performed on the samples: (i) differential scanning calorimetry (DSC) measurements using a DuPont 2000 Thermal Analyzer with a quench cooling accessory, the details of which were given in earlier studies;[20,21] (ii) frequency domain dielectric relaxation measurements using an HP4284A Precision LCR Meter in the frequency range 20–10^6 Hz; and (iii) time domain dielectric relaxation measurements in the time window of 0.01–1000 s using a Keithley Model No. 617 Programmable Electrometer. The discharging current in the sample (in the form of a capacitor) was sampled using a DSO-2200 instrument (Link Instruments, Inc., USA) from the 2 V analogue

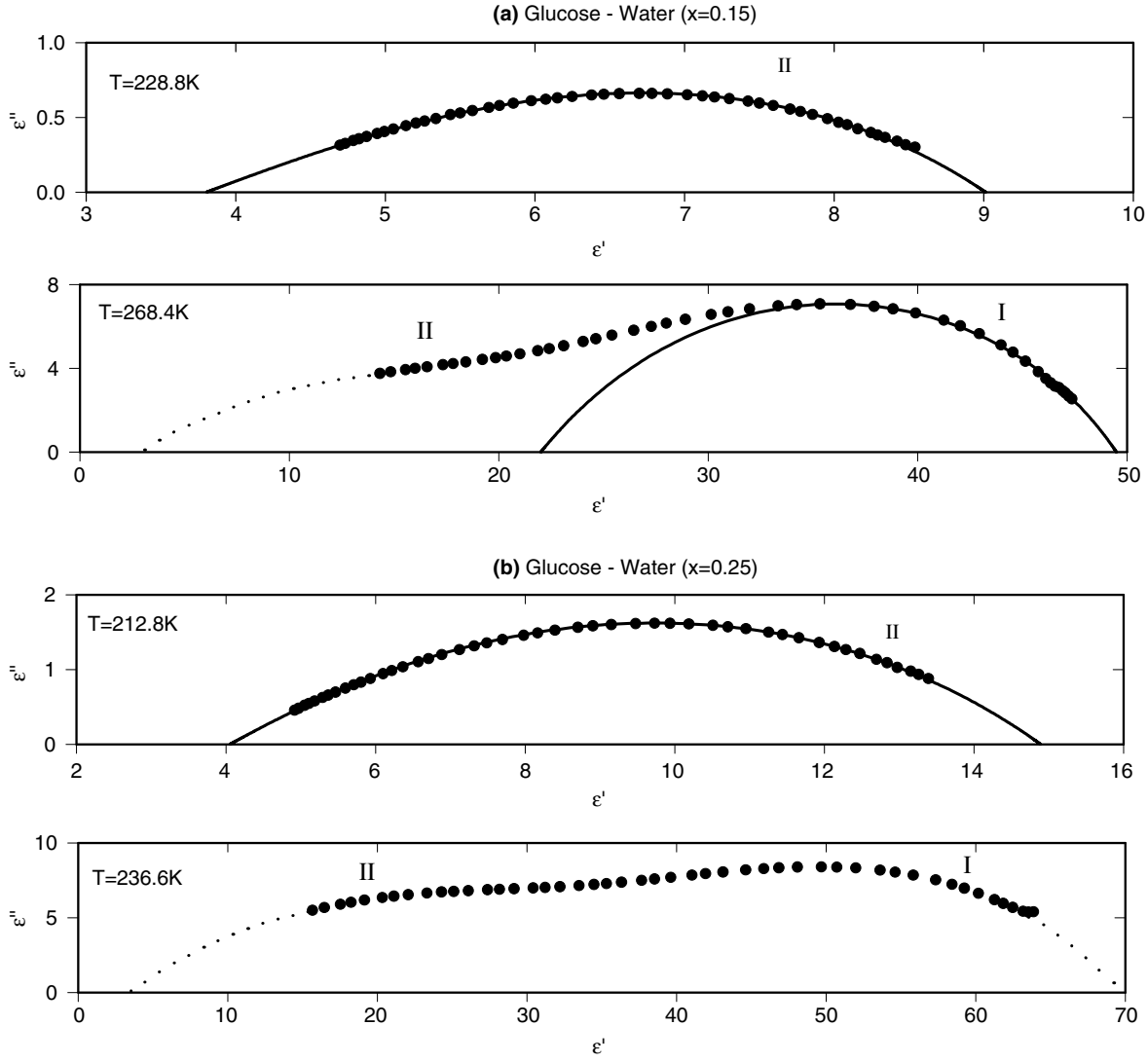

Figure 2. Cole–Cole diagrams (in the frequency range of 20 Hz–1 MHz) for the glucose–water mixtures. Solid lines are fits to Eq. 1, and the corresponding parameters are: (a) $x = 0.15$; $T = 228.8$ K ($\alpha_{HN} = 0.618$, $\beta_{HN} = 0.595$, $\varepsilon_0 = 9.01$ and $\varepsilon_\infty = 3.80$); $T = 268.4$ K ($\alpha_{HN} = 0.375$, $\beta_{HN} = 0.900$; $\varepsilon_0 = 49.50$ and $\varepsilon_\infty = 22.00$); (b) $x = 0.25$; $T = 212.8$ K ($\alpha_{HN} = 0.602$, $\beta_{HN} = 0.802$, $\varepsilon_0 = 14.89$ and $\varepsilon_\infty = 4.05$). The dotted lines on the high-frequency side show approximate path of Cole–Cole diagram drawn with the help of ε_∞ values.

voltage output and Preamp Out of Electrometer. The DSO-2200 could sample the voltage with the rates as high as 1 Mega samples/s. A high-speed electronic switch, HV220P (Supertex, Inc., USA), was used for switching purposes and could handle a charging voltage of up to 220 V. The complex permittivity was calculated by taking Discrete Fourier Transform (DFT) of the discharging current. Prior to these measurements, we measured the transient current for 2-ethylhexanol[35] and pure acetone clathrate hydrate[36] to check the accuracy of our setup. The peak loss frequency was found to be same within experimental error, and dielectric strength was found to be within 5% of the values. However, because of the limitation of the voltage resolution of the DSO-2200, we could not exactly determine the shape of the relaxation spectra. The details of the dielectric cell the accuracy and temperature control were the same as described in earlier study.[20,21] In the case of the DSC measurements, the glass-transition temperature T_g data given in this paper are an average of five runs.

3. Results

3.1. General considerations

Prior to the dielectric investigation, we have used the DSC technique to thoroughly investigate the crystallization and glass-transition behaviour of the samples, the results of which are given in Table 1. (Some of these results have already been reported in our earlier Ref. 21.) The dielectric measurements reported in this report are performed as a function of frequency over a range of fixed temperature. For the sake of convenience, we have divided this section into subsections as follows.

3.2. Aqueous solutions of glucose

Glucose–water mixtures can be supercooled easily without any crystallization for $x \leqslant 0.25$, where x is the weight fraction of water in the solution. These mixtures have been studied over a frequency interval of 5 Hz–4 MHz by earlier workers.[17–19,25–28,37] The T_gs of mixtures for $x = 0.15$ and 0.25 were found[37] to be 232.5 and 206.4 K, respectively, where x corresponds to the weight fraction of water in the solution. We have studied these samples over a much wider frequency of 10^{-3}–10^{6} Hz. For preparation of both of the mixtures studied here, the mixtures of solid glucose and water were heated to about 350 K. Precise weight measurements were made before and after heating to ensure no loss of water during heating. Above room temperature, there is a large contribution from dc conductivity to the dielectric loss, and appropriate analysis was carried out to get the dipolar loss. Shown in Figure 1 are the dielectric loss curves for glucose–water mixtures (for $x = 0.15$ and 0.25) at test frequencies of 0.028 Hz and 1 kHz. Plots at 0.028 Hz show clearly two processes that can be identified as process I and process II, which could not be seen as separate processes at 1 kHz, as they overlap in

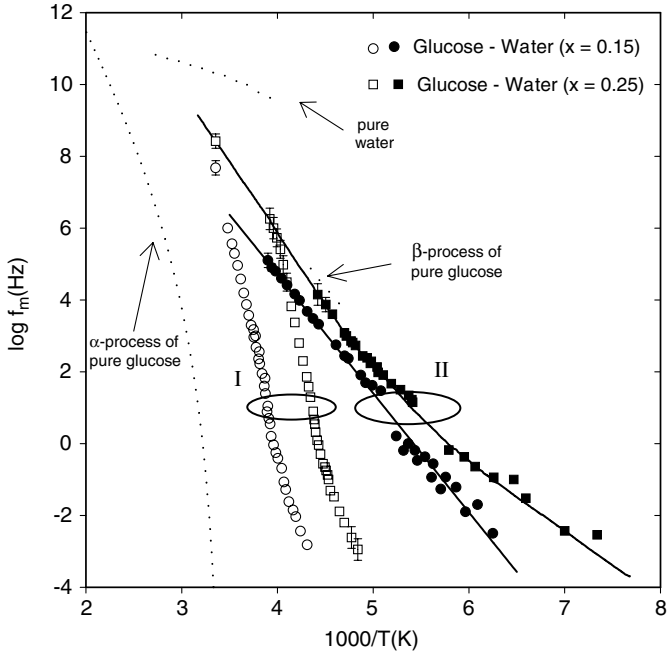

Figure 3. Arrhenius plot for glucose–water mixtures. Also shown for the sake of comparison the f_m values (dotted lines) of pure glucose[39] (both α- and β-processes) and water.[48–50] Also shown are the room temperature f_m values for glucose mixtures (shown as open symbols) estimated from the data given in Refs. 17 and 19. Solid lines drawn through the points are a guide to the eye. The uncertainties at high temperature in the f_m values of process I, especially in case of $x = 0.25$, are because of the presence of process II of much larger magnitude (also see Fig. 2b).

frequency. Shown in Figure 2, are the Cole–Cole diagrams for the same. Instead of the usual logarithmic plot of ε'' versus frequency, we preferred to use the complex plane representation to highlight the difficulty in resolving the two processes above T_g. The dielectric data have been analyzed using the Havriliak–Negami[38] (HN) equation given by

$$\frac{\varepsilon^*(f)-\varepsilon_\infty}{\varepsilon_0-\varepsilon_\infty}=\left(1+\mathrm{i}\left(\frac{f}{f_0}\right)^{1-\alpha_{HN}}\right)^{-\beta_{HN}} \quad (1)$$

where ε_0, ε_∞ are the limiting dielectric constants at low and high frequencies, respectively, and f_0 is the mean relaxation frequency. [The peak frequency f_m is obtained with the help of the relation between f_0, α_{HN} and β_{HN} as given in our earlier publication[20] where $f_m = f_0\left[\frac{k'}{\cos(\alpha\pi/2)-\sin(\alpha\pi/2)\cdot k'}\right]^{\frac{1}{(1-\alpha)}}$, where $k'=\tan\left(\frac{(1-\alpha)\pi}{2(1+\beta)}\right)$.] The above equation reduces to the well-known Debye equation when $\alpha_{HN}=0$, $\beta_{HN}=1$; to the Cole–Davidson (CD) equation when $\alpha_{HN}=0$; and to the Cole–Cole (CC) equation when $\beta_{HN}=1$. The parameter α_{HN} is a measure of the distribution of relaxation times in the sample, and the parameter β_{HN} is a measure of cooperativity among the molecules. We have also determined the ε_0 values in all the mixtures up to a temperature of 368 K, to estimate the total dielectric strength $\Delta\varepsilon$ $(\varepsilon_0-\varepsilon_\infty)$.

The Cole–Cole diagrams are analyzed using Eq. 1 to get the f_m values. With increasing water content, process II becomes more dominant as can be seen in Figure 2b, and because of this reason processes I and II could not be resolved very well above T_g. In case of glucose–water ($x=0.15$), process I is found to be more symmetric than process II. Corresponding Arrhenius plots are shown in Figure 3. The T-dependence of f_m values corresponding to process I, is found to follow the power-law equation[39] given by

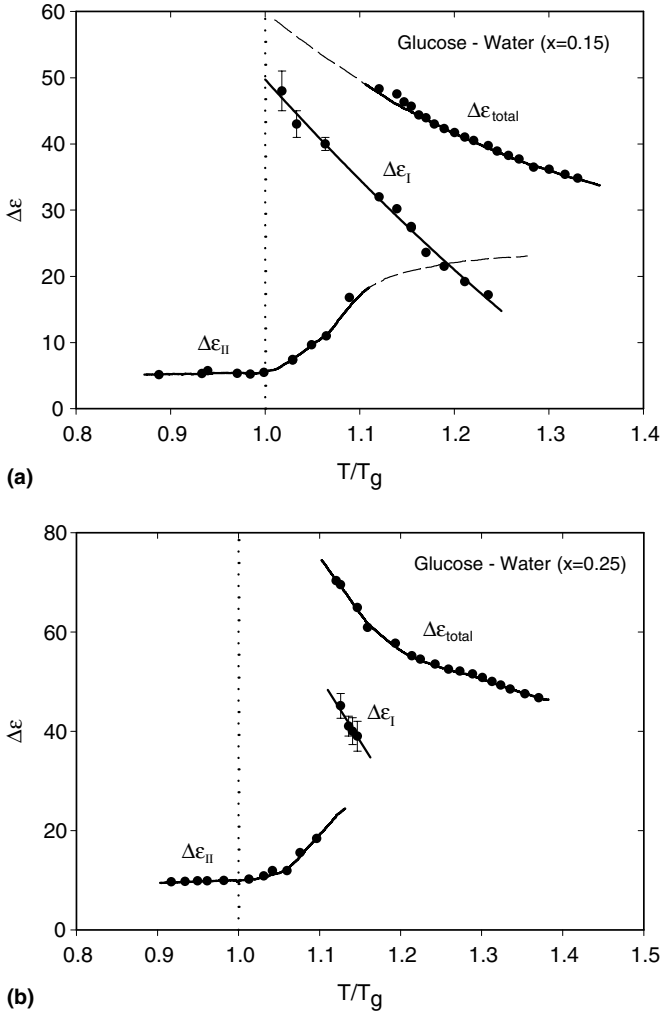

Figure 4. Variation in $\Delta\varepsilon$ values with temperature (normalized to the corresponding T_g) in mixtures of glucose–water for (a) $x=0.15$ and (b) $x=0.25$. Solid lines are a guide to the eye. Dashed lines in (a) correspond to the approximate extrapolations made on the assumption $\Delta\varepsilon_{total}=\Delta\varepsilon_I+\Delta\varepsilon_{II}$.

$$f_{m,I} = A\left(\frac{T - T'_g}{T'_g}\right)^r \quad (2)$$

where T'_g is the zero relaxation frequency temperature (i.e., the limiting glass transition for infinite cooling rate) and r is the dynamic exponent. The T-dependence of f_m values corresponding to process II is analyzed using the Arrhenius equation,[40] which is given as follows:

$$f_{m,II} = f_{0,II}e^{-E_{II}/RT} \quad (3)$$

In this equation, E stands for the apparent activation energy per mole, $f_{0,II}$ is the preexponential factor.

Unfortunately, we could not fit the f_m values corresponding to process I to Eq. 2 because of the uncertainty in the f_m values (see Fig. 3). If we use Eq. 3, it gives $f_0 = 7.9 \times 10^{46}$ Hz and $E = 224.56$ kJ/mol for the sample with $x = 0.15$ and $f_0 = 3.39 \times 10^{50}$ Hz with $E = 216.59$ kJ/mol for the sample with $x = 0.25$. The high values of f_0 in excess of 10^{13} Hz (lattice vibrational frequency) by many orders, is a clear indication of cooperative process characteristic of the α-process in supercooled liquids. The corresponding high (apparent) E values (calculated above) also confirm this view. For comparison purposes, we have also shown the Arrhenius plots of pure components in the same figure. Although, we are not able to resolve the two processes for the glucose–water ($x = 0.25$) sample, we are able to calculate peak loss frequency with confidence. The large uncertainty in the f_m values on the high-T side, especially in the sample with $x = 0.25$, is because of unusual broadness of the relaxation spectra due to the overlap of processes I and II. In Figure 4, the corresponding variation of dielectric strength ($\Delta\varepsilon$) with temperature is depicted. The important feature of this diagram is a noticeable increase in the dielectric strength of process II above T_g. We could not determine directly the $\Delta\varepsilon_{II}$ values of process II at higher temperatures, and, hence, we have obtained $\Delta\varepsilon_{II}$ values at higher temperatures after subtracting the dielectric strength of process I from the total dielectric strength. For the glucose–water ($x = 0.25$) sample, process I could be resolved only approximately over a very narrow temperature range, and, hence, the corresponding values of $\Delta\varepsilon$ are very approximate as shown by the large error bars in Figure 4b.

3.3. Aqueous solutions of PEG200

The second set of materials we have studied with water consists of low-molecular-weight polymeric ethylene glycols. The phase diagram of PEG–water mixtures

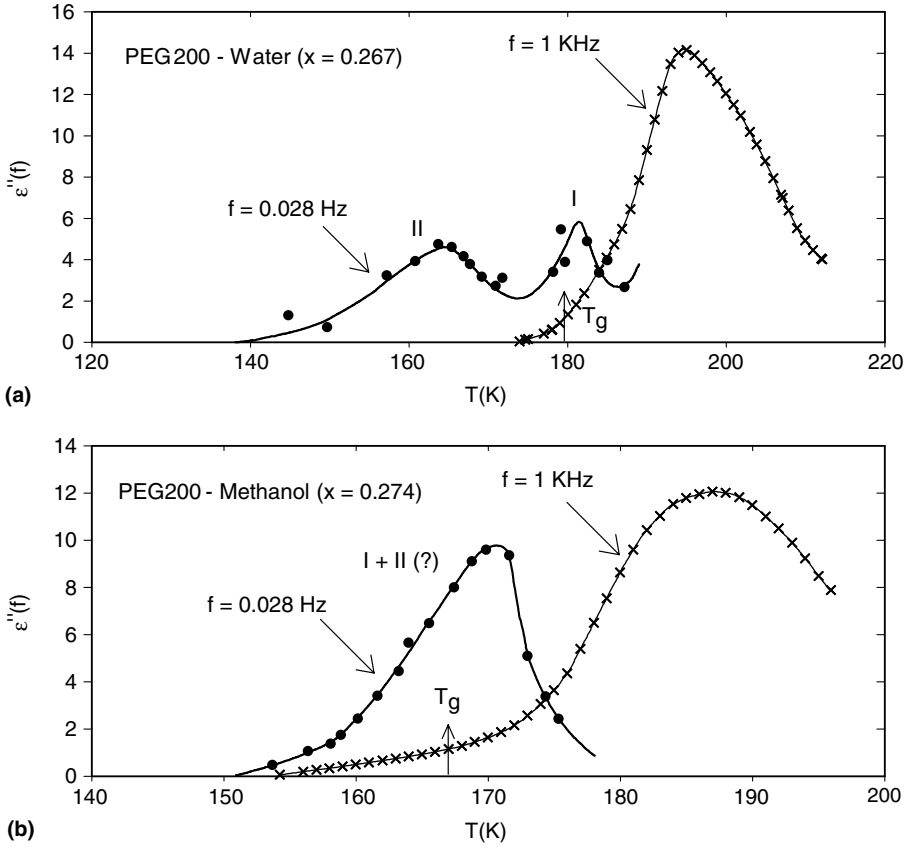

Figure 5. Isochronal plots of the imaginary part of the dielectric constant for (a) PEG200–water ($x = 0.267$) and (b) PEG200–MeOH ($x = 0.274$) at test frequencies of 0.028 Hz and 1 kHz. The experimental points for 1 kHz are not shown in the diagram for the sake of clarity. The lines drawn through the points are a guide to the eye.

was studied earlier[21] by one of us. The aqueous solutions of PEG200 can be supercooled easily for $x \leqslant 0.30$ (where x is the weight fraction of water) and could be studied in their supercooled states without any intervention of crystallization. We have studied PEG200–water ($x = 0.267$), whose T_g(DSC) is 178.9 K. The variation of dielectric loss with temperature for PEG200–water mixture at 0.028 Hz and 1 kHz is shown in Figure 5a, which clearly shows the presence of a sub-T_g process (II) along with the primary process (I). The Cole–Cole diagrams for process II are found to be symmetric in nature, and the values of parameter α_{HN} were found to be in the range of 0.33–0.46. (Corresponding diagrams are discussed in detail in our earlier publication.[21]) We have also studied the mixtures of PEG200 and methanol (MeOH) to compare the dynamics of the water molecule with another hydrogen-bonded system. The T_g of this system, PEG200–MeOH, $x = 0.274$ as determined by DSC, is 166.4 K, where x is the weight fraction of the alcohol in the liquid mixture. The corresponding dielectric behaviour is shown in Figure 5b. Arrhenius plots for the two systems are shown in Figure 6. One can notice the bifurcation of process II in case of the PEG200–water system well above T_g. The PEG200–MeOH system shows two processes in the low-T data near T_g, but the same could not be seen at higher temperatures. In Figure 7, $\Delta\varepsilon$ variation with temperature for the PEG200–water mixture is plotted along with PEG200–MeOH for comparison. It can be seen very clearly in Figure 7a that $\Delta\varepsilon$ values for process II in case of the PEG200–water system show a rapid increase above T_g and finally follow a liquid-like (i.e., inverse relationship with temperature) behaviour at high temperatures.

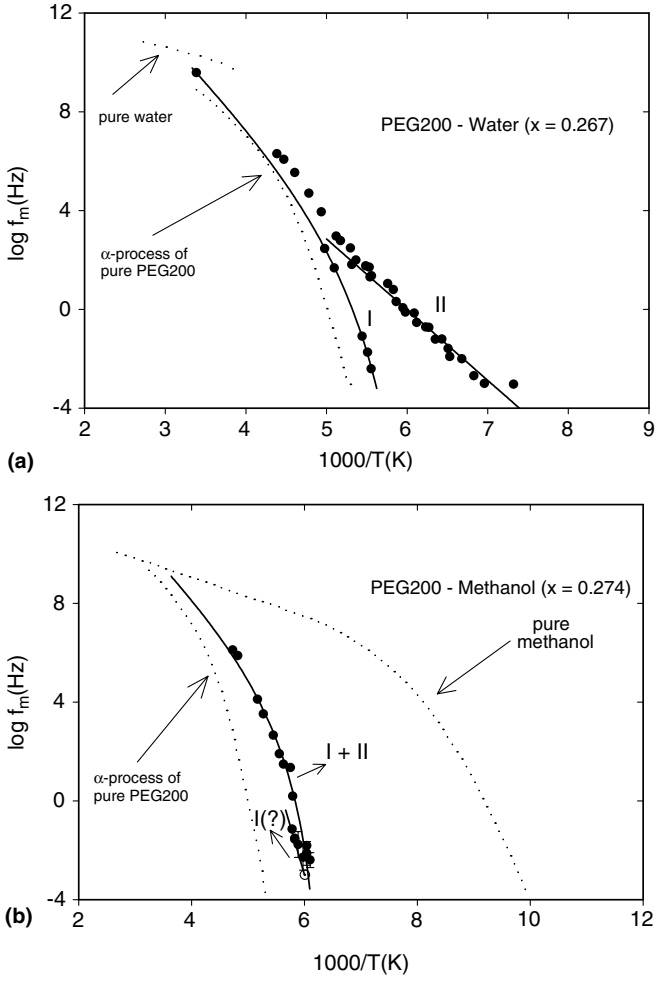

Figure 6. Arrhenius plots for (a) PEG200–water ($x = 0.267$) and (b) PEG200–MeOH ($x = 0.274$). The straight line in (a) for process II is an Arrhenius fit, and the corresponding parameters are given in Table 1. Also shown are the f_m values of pure components for PEG200,[21] water,[48–50] and MeOH[40] and the room temperature data for PEG200–water estimated from the data given in Refs. 6 and 51 for the purpose of comparison. One may also notice the presence of two non-Arrhenius processes in (b) PEG200–MeOH in the vicinity of T_g. The Arrhenius curve for pure MeOH is generated with the help of T_g value ($T_g = 103$ K) and from f_m values reported in Refs. 20 and 48. The thick lines on process I correspond to Eq. 2 with (a) $\log A = 10.88$, $r = 12.69$, and $T_g' = 165.0$ K (for PEG200–water) and (b) $\log A = 10.37$, $r = 9.42$, and $T_g' = 158.8$ K (PEG200–MeOH).

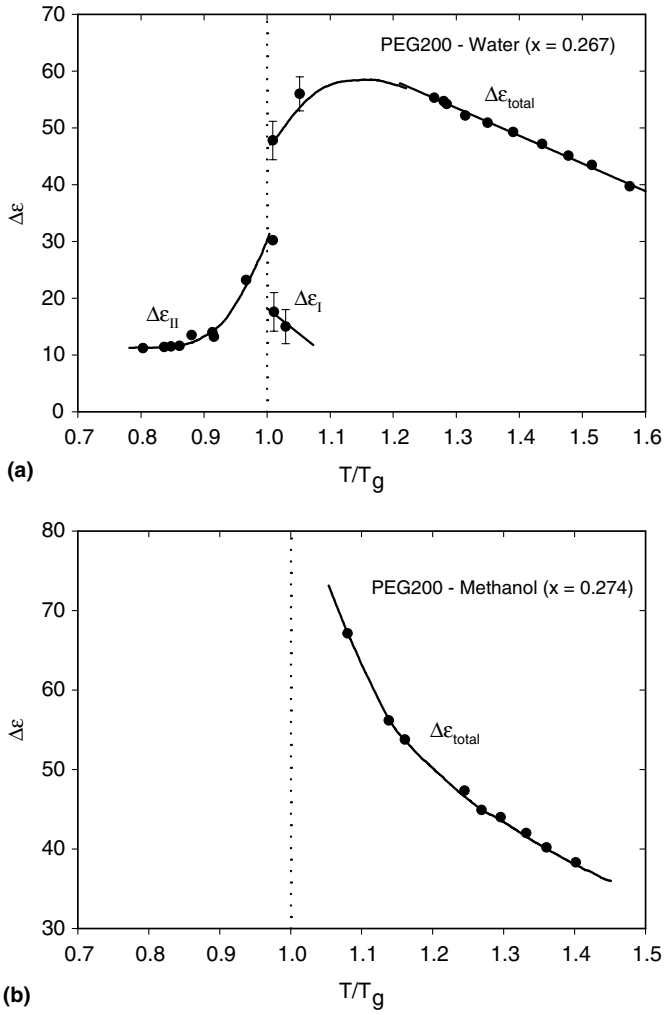

Figure 7. Variation of dielectric strength with temperature (normalized to the corresponding T_g) for (a) PEG200–water ($x = 0.267$) and (b) PEG200–MeOH ($x = 0.274$). The solid lines are a guide to the eye.

3.4. Aqueous solutions of PEG600

The phase diagram of aqueous mixtures of PEG600 was studied by one of us earlier,[21] but the T-variation of sub-T_g process was not determined below T_g. Aqueous solutions of PEG600 could be supercooled for $0.25 \leqslant x \leqslant 0.48$ without any problem of crystallization. We have studied the PEG600–water ($x = 0.404$), the T_g(DSC) of which is found to be 194.4 K. Figure 8 shows the relaxation processes observed in the PEG600–water system. The Cole–Cole diagrams could be well represented by depressed Cole–Cole arcs, and the parameter α_{HN} is found to be close to 0.4. (See Table 1. Some additional details can also be found in our earlier article.[21]) Figure 8a depicts the Arrhenius plot for the PEG600–water system, and the corresponding $\Delta\varepsilon$ values are plotted in Figure 8b. Unlike the other systems that we have studied, in the present report, processes I and II continue to exist as two separate processes up to room temperature, and interestingly, even process II shows non-Arrhenius behaviour above T_g. However, the dielectric strength of process I could not be tracked with temperature because of the presence of the dominant process II, and we have shown only a single point (with error bar) in Figure 8b to give the reader some idea of dielectric strength of process I.

3.5. PVP–water mixture

PVP is a highly crystalline substance but shows a glass transition at 326 K. The aqueous mixtures of PVP were studied earlier[6] at room temperature and showed two processes. The higher frequency process was attributed to reorientation of water molecules, and the low-frequency process was found to be due to micro-Brownian motion of the PVP chain. Aqueous solutions of PVP could not be supercooled completely as some amount of crystallization was always present. (The T_g

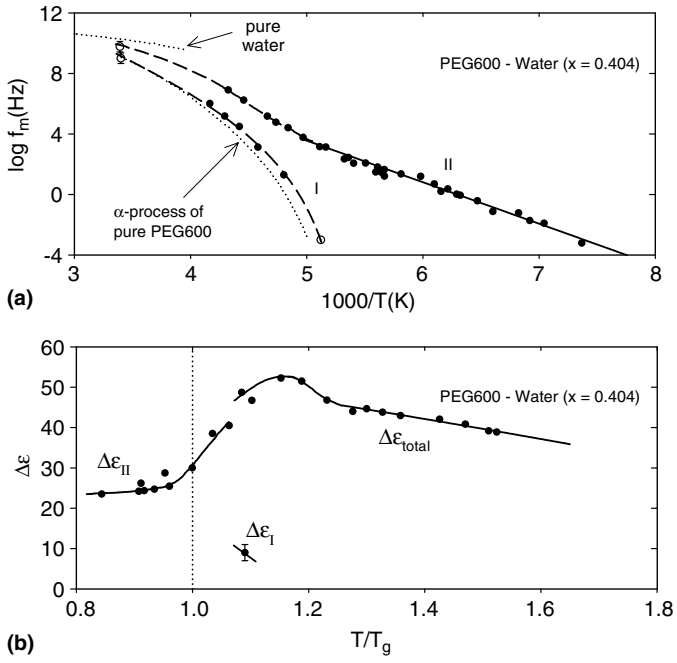

Figure 8. PEG600–water ($x = 0.404$): Shown in the figure are (a) the Arrhenius plot and (b) the variation of dielectric strength ($\Delta\varepsilon$) with temperature (normalized to the corresponding T_g). Also shown in (a) (by dotted lines) are the pure component values taken from Refs. 48–50,21,51. The straight line on the process II is Arrhenius-fitted, and the corresponding parameters are given in Table 1. The thick line in process I is given by Eq. 2 with $\log A = 11.81$, $r = 10.99$, and $T'_g = 187.0$ K. Because of the dominance of process II, the $\Delta\varepsilon$ corresponding to the process I could not be resolved (see part (b)).

determined from various runs from DSC is assigned to be 193 ± 6 K.) In an aqueous solution of PVP, the entire dispersion is mainly due to the sub-T_g process, and the contribution from the main relaxation is not appreciable. The corresponding dielectric loss versus frequency curves at various frequencies do not show any appreciable change at T_g (see Ref. 21 for further details). In order to resolve unclear process I, we have subtracted the dc loss from the total dielectric loss. If we make use of the room temperature data of others,[6] an approximate path of process I could be drawn as shown in Figure 9a. PVP is soluble, not only in water, but also in low-molecular-weight alcohols such as MeOH. This mixture also revealed a weak process I that could be resolved after subtracting dc loss from the total dielectric loss as in the previous case. Together with the available room-temperature data, an approximate path of process I could be deduced as shown in Figure 9b. We have not shown a variation of dielectric strength in case of the PVP–water mixture because of large uncertainties in $\Delta\varepsilon$ values and the problem of crystallization on increasing the temperature (see also Ref. 8 for details on crystallization).

In order to get an insight about the nature of mechanism of the sub-T_g process (or process II) in the aqueous solutions and its relation to the free water, we have depicted the corresponding f_m values in Figure 10, along with that of pure water values.

4. Discussion

Mashimo et al.[17] have performed detailed measurements over a frequency range of 1 MHz–20 GHz on a sample of the aqueous solution of glucose with $x = 0.25$. Only one relaxation process was found at room temperature with $\log f_m(\text{Hz}) = 8.41$, and the relaxation is of HN-type (Eq. 1) with $\alpha_{HN} = 0.252$ and $\beta_{HN} = 0.650$. Our measurements detailed in Figures 1–4 reveal that the above relaxation splits into two processes on lowering the temperature. The process designated as I actually corresponds to the so-called α-process, which is non-Arrhenius and gets arrested at T_g, whereas the second process designated as II is Arrhenius and continues to the sub-T_g region. Interestingly, process II is found to increase in magnitude with increase in the weight fraction of water in the sample, and it is more or less symmetrical in its spectral dependence. Its spectral shape parameters and the corresponding activation energy shown in Table 1, are very similar to that of the 'confined water' relaxation [or the Johari–Goldstein (JG) relaxation] found[21,32] below T_g in many aqueous solutions. Moreover, from the general trend of the T-dependence of $\Delta\varepsilon$ shown in Figure 4b, one can expect the contribution of process I at room temperature to the total dielectric strength to be small, and, hence, all the polarization is expected to be from process II. Interestingly, the room temperature point of Mashimo et al.[17]

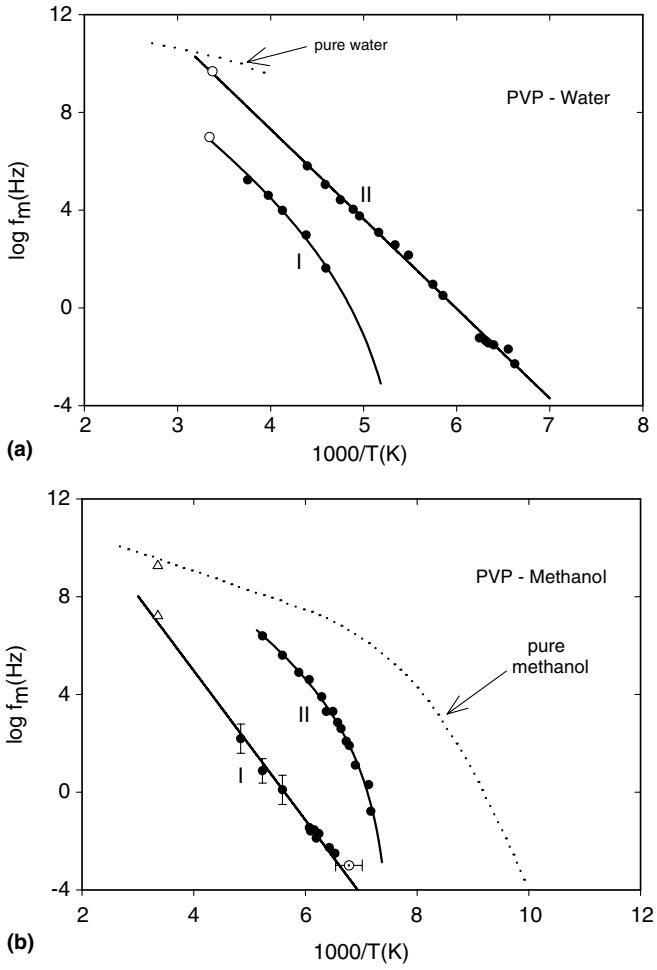

Figure 9. Arrhenius plots for (a) PVP–water and (b) PVP–MeOH systems. The thick lines in process I in (a) and process II in (b) are given by Eq. 2 with; (a): $\log A = 8.74$, $r = 10.40$, $T_g' = 179.8$ K (in PVP–water) and (b): $\log A = 9.10$, $r = 7.71$, $T_g' = 131.96$ for (PVP–MeOH). The straight line in process I in (b) is Arrhenius-fitted with $f_0 = 1.54 \times 10^{17}$ Hz and $E_0 = 58.52$ kJ/mol. Horizontal error bars show the uncertainty in the composition,[21] and hence the glass-transition temperature due to partial crystallization during cooling. Also shown are the corresponding f_m values for the pure components (water and MeOH). The points shown as open symbols correspond to the data of Mashimo and co-workers[6] at room temperature. It should be noted that process I is a weak process, and there is a large uncertainty in its locus (see Ref. 21 for details).

(discussed in the beginning of this section) falls on the extrapolated Arrhenius line of process II (see Fig. 3), indicating that it is due to the confined water clusters, which suggests that there is a compatibility of the ring-like structure of glucose with the (hexagonal) ring-like structure of the water. This inference agrees well with interpretation of the dielectric data taken at different concentrations on the aqueous solutions of glucose by Mashimo et al.[17] and by Fuchs and Kaatze.[19] Another interesting observation is that the $\Delta\varepsilon_{II}$ shows a rapid change above T_g, and correspondingly, there is a large increase in the magnitude of $\Delta\varepsilon_I$ on approaching T_g, indicating that water molecules (the dominant dipoles) are increasingly bound to the glucose molecules. The glass-transition event at T_g is due to the kinetic freezing of the 'above structure'; however, water molecules located far away from the glucose molecules not bound to the above structure will continue to enjoy rotational freedom even below T_g, which is realizable as process II.

The situation is different in the case of PEG, which has H-bonding sites only at the ends of the molecule, and hence, one can expect the amount of 'bound' water to decrease with an increase in molecular weight. Therefore, one can expect process I to decrease, and hence, process II is expected to dominate the dielectric measurements. This is exactly what we infer from a comparison of the dielectric strength associated with processes I and II shown in Figures 5a and 7a with Figure 8b for the cases of PEG200 and PEG600. On the other hand, the relaxation frequencies associated with process I are expected to decrease as the size of the molecular segment involved in the glass-transition process increases in size due to an increase in molecular weight of the polymer (PEG in the present context), and hence, the relaxation frequencies corresponding to the processes I and II are also expected to differ more from each other. This is exactly what we see in our Arrhenius plots shown in Figures 6a and 8a, and interestingly, so wide is the

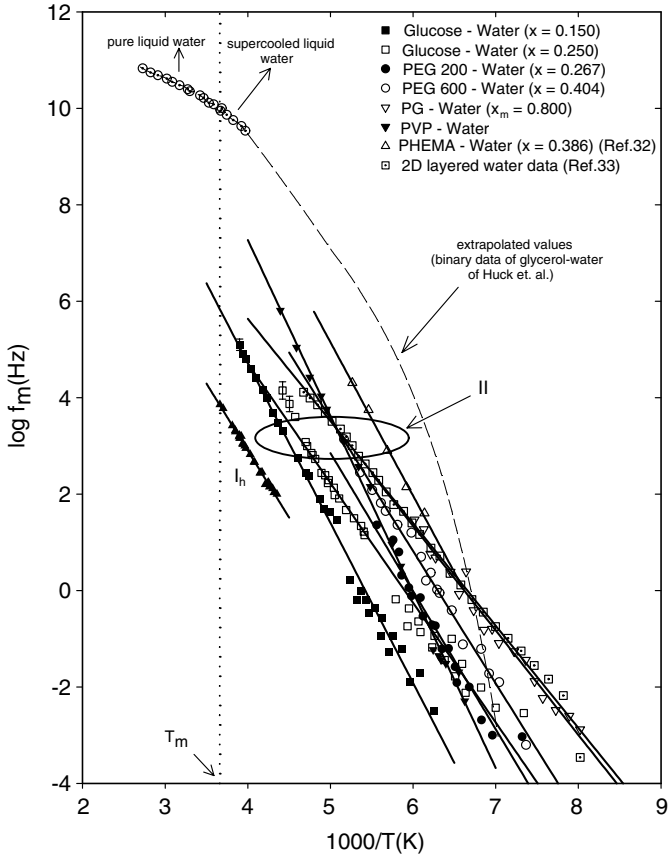

Figure 10. Temperature variation of peak loss frequency (f_m) for process II in several binary aqueous mixtures. Also shown in the plot are the data corresponding to pure water[48–50] (on the high-T side) and hexagonal ice[43,44] (I_h) in the intrinsic region. The dotted line on the water curve corresponds to the bulk water in its supercooled region estimated by Huck et al.[52] by the extrapolation of the data on glycerol–water systems, which also terminates at T_g, which is 138 K (estimated from binary solution data and for the hyperquenched water sample[53]).

separation of the two processes that even in the room temperature data of Mashimo and co-workers,[11–17] they are noticeable as two distinct processes in higher PEG solutions. So is the case with the PVP–water mixture shown in Figure 9a. Another interesting aspect of our measurements is that the total dielectric strength (i.e., $\Delta\varepsilon_I + \Delta\varepsilon_{II}$) shows a rapid fall in its magnitude on approaching T_g from the higher temperature side (see, Figs. 7a and 8b). This indicates that there is a large hindrance to the rotation of the water molecules, especially the ones associated with process II.

The most interesting point of our observations is that when water is replaced with MeOH in the mixtures, instead of process II, which looked Arrhenius-like in aqueous mixtures, we now get a non-Arrhenius branch characteristic of a phase-separated liquid, as shown in Figures 6b and 9b. Non-Arrhenius curves of the kind shown in Figures 6b and 9b are typical of the behaviour exhibited[41,42] in mixtures of two dissimilar liquids like an alcohol and an alkyl halide. Two non-Arrhenius branches in the above case correspond to the two well-separated liquids phases rich in the component liquids. Thus, it is tempting to identify the high-frequency branch in the above two figures with the MeOH-dominant phase. Interestingly, this branch more or less freezes at almost the (same) T_g along with process I, indicating that this alcohol-rich branch, that is, process II, is not completely free and is getting very much hindered as far as the rotation of the molecules is concerned.

The above observation clearly hints at a possibility that process II seen in aqueous solutions can also be treated as corresponding to confined water in which the water molecules are getting hindered to varying degrees. This hindrance is expected to be increasingly stronger in the order: higher PEGs, lower PEGs, and glucose as seen in the previous paragraphs. This raises a fundamental question: will a pure water phase always reveal itself as an Arrhenius process (all the time) as opposed to non-Arrhenius behaviour of other liquids? In order to answer this question, we have compared in Figure 10 the relaxation rates corresponding to 'confined water', that is, process II, in different matrices, with that of pure water (absolutely free water) for which the dielectric relaxation rates are available down to ~235 K. Also shown in the same figure are the data cor-

responding to the intrinsic region of hexagonal ice (I_h). The relaxation frequencies are always higher than that of water relaxation in I_h, and the activation energy, though completely not independent of the solvent, is comparable to that of I_h, which is ~55 kJ/mol.[43,44] This leaves a distinct possibility that the curve for process II in Figure 10 may become steeper enough to meet the high-T pure water branch if the interactions between the water molecules and the solvent are low enough, although the 2D-layered water data rule out this possibility. It is interesting to note that a major portion of the curves shown in Figure 10 are all located between the curves of I_h and the one expected for pure water (based on the binary data and the DSC T_g).

5. Conclusions

We have observed that the sub-T_g process designated as process II in all the above experiments is Arrhenius below the bifurcation temperature, and it is characterized by a more or less symmetric distribution of relaxation times. It can be attributed to 'confined water' (not bound to the structure that is freezing at T_g). Although it is tempting to identify it with a strong liquid as was first suggested by Angell,[45–47] for water in its supercooled state, some caution must be exercised as these water molecules are found to be hindered to varying degrees. In this context, we wish to point out that in the case of aqueous solutions of glycerol,[21] dimethyl sulfoxide[20] (DMSO), ethylene[20] and propylene glycols,[21] where the interaction between water and the solvent molecules was proved to be much stronger than the above cases (shown in Fig. 10), the corresponding relaxation frequencies of process II are found to be located in a narrow frequency range of 10^{-1}–10^{-3} Hz (not shown in Fig. 10) with an apparent activation energy much smaller than that of the cases shown in Figure 10. This leaves a distinct possibility that the curves corresponding to process II might become non-Arrhenius if the interaction between water and the host matrix become negligibly small. Why we leave this possibility open is that something drastic should happen in supercooled water in a narrow temperature interval of 200–235 K for the curve corresponding to pure water to meet in a smooth fashion one of the curves of the kind shown in Figure 10, although there is no evidence of it in the dielectric measurements made close to 235 K.

Acknowledgments

One of the authors, Madhusudan Tyagi, gratefully acknowledges the financial assistance from CSIR, India, during the course of the present work.

References

1. Franks, F. *J. Solution Chem.* **1995**, *24*, 1093–1097.
2. Slade, L.; Levine, H. In *Advances in Food and Nutrition Research*; Kinsella, J. E., Ed.; Academic Press: San Diego, 1994; Vol. 38.
3. Angell, C. A.; Bressel, R. D.; Green, J. L.; Kanno, H.; Oguni, M.; Sare, E. J. *J. Food Eng.* **1994**, *22*, 115–142.
4. Boutron, P.; Peyridieu, J. F. *Cryobiology* **1994**, *31*, 367–373.
5. Van Den Abbeel, E.; Van Der Elst, J.; Van Der Linden, M.; Van Steirteghem, C. *Cryobiology* **1997**, *34*, 1–12.
6. Shinyashiki, N.; Asaka, N.; Mashimo, S.; Yagihara, S. *J. Chem. Phys.* **1990**, *93*, 760–764.
7. Shinyashiki, N.; Yagihara, S.; Arita, I.; Mashimo, S. *J. Phys. Chem. B* **1998**, *102*, 3249–3251.
8. Shinyashiki, N.; Matsumura, Y.; Miura, N.; Yagihara, S.; Mashimo, S. *J. Phys. Chem.* **1994**, *98*, 13612–13615.
9. Shinyashiki, N.; Yagihara, S. *J. Phys. Chem. B* **1999**, *103*, 4481–4484.
10. Asaka, N.; Shinyashiki, N.; Umehara, T.; Mashimo, S. *J. Chem. Phys.* **1990**, *93*, 8273–8275.
11. Mashimo, S.; Umehara, T.; Redlin, H. *J. Chem. Phys.* **1991**, *95*, 6257–6260.
12. Gestblom, B.; El-Samahy, A.; Sjoblom, J. *J. Solution Chem.* **1985**, *14*, 375–392.
13. Tombari, E.; Chryssikos, G.; Gestblom, B.; Cole, R. H. *J. Mol. Liq.* **1989**, *43*, 53–69.
14. Kuwabara, S.; Umehara, T.; Mashimo, S.; Yagihara, S. *J. Phys. Chem.* **1988**, *92*, 4839–4841.
15. Mashimo, S.; Kuwabara, S.; Yagihara, S.; Higasi, K. *J. Phys. Chem.* **1987**, *91*, 6337–6338.
16. (i) Ozawa, R.; Komori, T.; Umetsubo, D.; Chiba, A.; Nozaki, R. (poster: Po-Sa 33) and (ii) Wakatsuki, M.; Minogichi, A.; Nozaki, R. (poster: Po-Su 29): *Abstr. 5th International Discussion Meeting on Relaxations in Complex Systems (SIDMRCS)*, USTL; Lille, France, 2005.
17. Mashimo, S.; Miura, N.; Umehara, T. *J. Chem. Phys.* **1992**, *97*, 6759–6765.
18. Stenger, J.; Cowman, M.; Eggers, F.; Eyring, E. M.; Kaatze, U.; Petrucci, S. *J. Phys. Chem. B* **2000**, *104*, 4782–4790.
19. Fuchs, K.; Kaatze, U. *J. Phys. Chem. B* **2001**, *105*, 2036–2042.
20. Murthy, S. S. N. *J. Phys. Chem. B* **1997**, *101*, 6043–6049.
21. Murthy, S. S. N. *J. Phys. Chem. B* **2000**, *104*, 6955–6962.
22. Sudo, S.; Shinyashiki, N.; Yagihara, S. *J. Mol. Liq.* **2001**, *90*, 113–120.
23. Sudo, S.; Shimomura, M.; Shinyashiki, N.; Yagihara, S. *J. Non-Cryst. Solids* **2002**, *307–310*, 356–363.
24. Sudo, S.; Shimomura, M.; Saito, T.; Kashiwagi, T.; Shinyashiki, N.; Yagihara, S. *J. Non-Cryst. Solids* **2002**, *305*, 197–203.
25. Chan, R. K.; Pathmanathan, K.; Johari, G. P. *J. Phys. Chem.* **1986**, *90*, 6358–6362.
26. Noel, T. R.; Parker, R.; Ring, S. G. *Carbohydr. Res.* **1996**, *282*, 193–206.
27. Noel, T. R.; Parker, R.; Ring, S. G. *Carbohydr. Res.* **2000**, *329*, 839–845.
28. Moran, G. R.; Jeffrey, K. R. *J. Chem. Phys.* **1999**, *110*, 3472–3483.
29. Nozaki, R.; Zenitani, H.; Minoguchi, A.; Kitai, K. *J. Non-Cryst. Solids* **2002**, *307–310*, 349–355.
30. Champion, D.; Maglione, M.; Niquet, G.; Simatos, D.; Le Meste, M. *J. Therm. Anal. Calor.* **2003**, *71*, 249–261.

31. Swenson, J.; Bellissent-Funel, M.-C. *Abstr., 5th International Discussion Meeting on Relaxations in Complex Systems (5IDMRCS)*, USTL; Lille, France, 2005, Abstr. B-FPG5 and B-FPG6.
32. Pathmanathan, K.; Johari, G. P. *J. Polym. Sci., Part B: Polym. Phys.* **1990**, *28*, 675–689.
33. Bergman, R.; Swenson, J. *Nature* **2000**, *403*, 283–286.
34. Swenson, J.; Bergmann, R.; Longeville, S. *J. Chem. Phys.* **2001**, *115*, 11299–11305.
35. Murthy, S. S. N. *Mol. Phys.* **1996**, *87*, 691–709.
36. Murthy, S. S. N. *J. Phys. Chem.* **1999**, *103*, 7927–7937.
37. Moran, G. R.; Jeffffey, K. R.; Thomas, J. M.; Stevens, J. R. *Carbohydr. Res.* **2000**, *328*, 573–584.
38. Havriliak, S.; Negami, S. *J. Polym. Sci., Polym. Symp.* **1966**, *no. 14*, 99–117.
39. Gangasharan; Murthy, S. S. N. *J. Phys. Chem.* **1995**, *99*, 12349–12354.
40. Hill, N. E.; Vaughan, W. E.; Price, A. H.; Davies, M. *Dielectric Properties and Molecular Behaviour*; Van Nostrand Reinhold: London, 1969.
41. Murthy, S. S. N.; Tyagi, M. *J. Solution Chem.* **2002**, *31*, 33–58.
42. Shahin, Md.; Tyagi, M.; Murthy, S. S. N. *J. Solution Chem.* **2003**, *32*, 155–177.
43. Murthy, S. S. N. *Phase Trans.* **2002**, *75*, 487–506.
44. Tyagi, M.; Murthy, S. S. N. *J. Phys. Chem. A* **2002**, *106*, 5072–5080.
45. Angell, C. A.; Shuppert, J.; Tucker, J. C. *J. Phys. Chem.* **1973**, *77*, 3092–3099.
46. Angell, C. A.; Tucker, J. C. *J. Phys. Chem.* **1980**, *84*, 268–272.
47. Angell, C. A. *J. Phys. Chem.* **1993**, *97*, 6339–6341.
48. Buckley, F.; Maryott, A. A. *Tables of Dielectric Dispersion Data for Pure Liquids and Dilute Solutions*; National Bureau of Standards Circular 589, 1958.
49. Hasted, J. B.; Shachidi, M. *Nature* **1976**, *262*, 777–778.
50. Ronne, C.; Thrane, L.; Astrand, P.; Wallqvist, A.; Mikkelsen, K. V.; Keiding, R. *J. Chem. Phys.* **1997**, *107*, 5319–5331.
51. Davies, M.; Williams, G.; Loveluck, G. D. *Z. Elektrochem.* **1960**, *64*, 575–580.
52. Huck, J. R.; Noyel, G. A.; Jorat, L. J. *IEEE Trans. Electr. Inst.* **1988**, *23*, 627–638.
53. Johari, G. P.; Hallbrucker, A.; Mayer, E. *Nature* **1987**, *330*, 552–553.